

# Polyfuran: A New Synthetic Approach and Electronic Properties

S. Glenis,<sup>†</sup> M. Benz,<sup>†</sup> E. LeGoff,<sup>†</sup> J. L. Schindler,<sup>‡</sup> C. R. Kannewurf,<sup>‡</sup> and M. G. Kanatzidis<sup>\*,†,§</sup>

Contribution from the Department of Chemistry and Center for Fundamental Materials Research, Michigan State University, East Lansing, Michigan 48824, and Department of Electrical Engineering and Computer Science, Northwestern University, Evanston, Illinois 60208

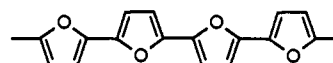
Received July 28, 1993\*

**Abstract:** Polyfuran films have been synthesized by electropolymerization of terfuran and investigated as a function of film preparation conditions in both the doped and undoped state. These films have been characterized by infrared spectroscopy, scanning electron microscopy, optical absorption, X-ray photoelectron spectroscopy, dc conductivity, and electron spin resonance measurements. The electrolyte anion (dopant) used for the preparation of these films heavily influences the  $\pi$ -conjugated system of the polymer backbone. Structural disorder and doping level depends on the nature of the electrolyte anion.  $\text{CF}_3\text{SO}_3^-$  was found to be the best dopant and to cause the least structural disorder or furan ring opening. Electrical conductivities as high as  $2 \times 10^{-3}$  S/cm were obtained in the  $\text{CF}_3\text{SO}_3^-$ -doped state. The temperature dependence of the electrical conductivity indicates a thermally activated process with semiconductor-like behavior. The charge transport properties are explained in terms of polaron and bipolaron states. The polymer band gap was measured at 2.35 eV.

## Introduction

Electronically conducting polymers continue to attract much attention from both a scientific and a technological perspective. In particular, polyheterocyclic polymers such as polypyrrole,<sup>1</sup> polythiophene,<sup>2,3</sup> polyselenophene,<sup>4</sup> and their derivatives constitute an important class among  $\pi$ -conjugated polymeric materials as they possess chemical and electrical stability in both the oxidized (doped) and neutral (undoped) state. The properties of these materials are promising for device fabrication<sup>5-7</sup> as well as anticorrosion coating applications for inorganic semiconductors.<sup>8</sup> In the five-membered heterocycles, the heteroatom provides two  $\pi$  electrons which, in addition to four  $\pi$  electrons from the carbon atoms, make up the aromatic system. Thus, the conjugated chains

## Chart I



and the electrical and optical properties of these polymers are highly influenced by the increasing electronegativity of the heteroatom.

Polyfuran is among the most ill-defined of conjugated polymers compared to polypyrrole and polythiophene. This polymer was claimed to have been obtained previously by electrochemical polymerization of furan, but the high voltage required for the electropolymerization (1.8–2.5 V) results in irreversible oxidation of the polymer.<sup>9</sup> The chemical and spectroscopic properties of the product are not consistent with the expected conjugated structure shown in Chart I. A polymer synthesized by a chemical method did not appear to be conjugated as it contained various hydrogenated units.<sup>10</sup> A significant degree of furan ring-opening occurs due to the drastic chemical conditions employed during synthesis and due to its lower aromaticity (higher energy) compared to pyrrole and thiophene. Thus, it appears that polyfuran, as shown in Chart I, may never have been prepared.

A material which appeared to be conjugated was reported to form from the cathodic reduction of 2,5-dibromofuran in the presence of a  $\text{Ni}^{2+}$  catalyst.<sup>11</sup> This polymer comes close to the expected description for polyfuran but it only formed in minute amounts due to blockage of the working electrode by the polymer, since inherent in this process is production of the undoped, insulating form. Thus, extensive characterization on this material could not be made.

In order to improve the electropolymerization process, and still maintain anodic conditions, we chose terfuran as the monomer because of its considerably lower oxidation potential (by  $\sim 1.5$  V) compared to furan itself. The lower oxidation potential of terfuran should provide considerably milder polymerization

<sup>†</sup> Michigan State.

<sup>‡</sup> Northwestern University.

<sup>§</sup> A. P. Sloan Foundation Fellow 1991–93 and Camille and Henry Dreyfus Teacher Scholar 1993–95.

\* Abstract published in *Advance ACS Abstracts*, December 1, 1993.

(1) (a) Kanazawa, K. K.; Diaz, A. F.; Gill, W. D.; Grant, P. M.; Street, G. B.; Gardini G. P.; Kwak, J. F. *Synth. Met.* **1980**, *1*, 329. (b) Street, G. B.; Clarke, T. C.; Krounbi M.; Kanazawa, K.; Lee, V.; Pfluger, P.; Scott, J. C.; Weiser, G. In *Molecular Crystals and Liquid Crystals*; Epstein, A. J., Conwell, E. M., Eds.; Gordon and Breach: New York, 1982; Vol. 83.

(2) (a) Tourillon, G.; Garnier, F. *J. Electroanal. Chem.* **1982**, *135*, 173. (b) Tourillon, G.; Garnier, F. *J. Electrochem. Soc.* **1983**, *130*, 2042. (c) Roncali, J. *Chem. Rev.* **1992**, *92*, 711.

(3) (a) Kobayashi, M.; Chen, J.; Chung, T. C.; Moraes, F.; Heeger, A. J.; Wudl, F. *Synth. Met.* **1984**, *9*, 77. (b) Chung, T.-C.; Kaufman, J. H.; Heeger, A. J.; Wudl, F. *Phys. Rev. B* **1984**, *30*, 702. (c) Patil, A. O.; Heeger, A.; Wudl, F. *Chem. Rev.* **1988**, *29*, 183.

(4) Glenis, S.; Ginley, D. S.; Frank, A. J. *J. Appl. Phys.* **1987**, *62*(1), 190.

(5) (a) Thackeray, J. W.; White, H. S.; Wrighton, M. S. *J. Phys. Chem.* **1985**, *89*, 5133. (b) Ofer, D.; Crooks, R. M.; Wrighton, M. S. *J. Am. Chem. Soc.* **1990**, *112*, 7869. (c) Wrighton, M. S. *Comments Inorg. Chem.* **1985**, *4*, 269–294.

(6) (a) Caja, J.; Kaner, R. B.; MacDiarmid, A. G. *J. Electrochem. Soc.* **1984**, *131*, 2744–2750. (b) Glenis, S.; Horowitz, G.; Tourillon, G.; Garnier, F. *Thin Solid Films* **1984**, *111*, 93. (c) Glenis, S.; Frank, A. J. *Synth. Met.* **1989**, *28*, C681. (d) Frank, A. J.; Glenis, S.; Nelson, A. J. *J. Phys. Chem.* **1989**, *93*, 3818. (e) Ohtani, A.; Abe, M.; Higushi, H.; Shimidzu, T. *J. Chem. Soc., Chem. Commun.* **1988**, 1545. (f) Shimidzu, A.; Yamataka, K.; Kohno, M. *Bull. Chem. Soc. Jpn.* **1988**, *61*, 4401. (g) Bradley, D. D. C. *Synth. Met.* **1993**, *54*, 401.

(7) (a) Kanatzidis, M. G. *Chem. Eng. News* **1990**, *68*, 36. (b) Friend, R.; Bradley, D. D. C.; Holmes, A. *Phys. World* **1992**, *Nov*, 42–46.

(8) (a) Noufi, R.; Frank, A. J.; Nozik, A. J. *J. Am. Chem. Soc.* **1981**, *103*, 1849. (b) Fan, F.-R. F.; Wheeler, B. L.; Bard, A. J.; Noufi, R. *J. Electrochem. Soc.* **1981**, *128*, 2042. (c) Frank, A. J.; Honda, K. *J. Phys. Chem.* **1982**, *86*, 1933.

(9) (a) Ohsawa, T.; Kaneto, K.; Yoshino, K. *Jpn. J. Appl. Phys.* **1984**, *23*, L663. (b) Nessakh, B.; Kotkowska-Machnik, Z.; Tedjar, F. *J. Electroanal. Chem.* **1990**, *269*, 263. (c) Tedjar, F. *Eur. Polym. J.* **1985**, *21*, 317.

(10) (a) Gardini, A. *Adv. Polym. Sci.* **1977**, *25*, 47. (b) Kang, E. T.; Neoh, K. G. *Eur. Polym. J.* **1987**, *23*, 719.

(11) Zotti, G.; Schiavon, G.; Comisso, N.; Berlin, A.; Pagani, G. *Synth. Met.* **1990**, *36*, 337.

conditions and yield a higher quality polymer. If good  $\alpha,\alpha'$  coupling selectivity were achieved, as well as a reduced ring-opening tendency in the polymer (by the decreased reactivity of the oxidized oligomer), a good quality material might be obtained. Using this synthetic approach, the previously restrictive polyfuran can now be prepared into stable films, in sufficient quantity, and this presents a new opportunity to study its properties.

In this paper, we report the synthesis, physicochemical studies, and charge transport characterization of polyfuran (PF). We have characterized this polymer by a variety of techniques, such as infrared and UV-visible spectroscopy, scanning electron microscopy (SEM), X-ray photoelectron spectroscopy (XPS), dc conductivity, and electron-spin-resonance (ESR) spectroscopy. In particular, we present evidence that this synthetic approach leads to a conjugated polymer, and we report the crucial effect of the electrolyte on the growth, composition, chemical stability, structural morphology, electronic properties, and transport processes of this polymer.

### Experimental Section

Terfuran was prepared as detailed elsewhere.<sup>12</sup> Prior to use, terfuran and solvents were distilled under reduced pressure. Polyfuran films were prepared by electrochemical oxidation of the monomer in a three-electrode one-compartment cell by potential sweeps between 0.0 and 1.0 V (versus SCE). The films were grown either on platinum or optically transparent tin-doped indium oxide (ITO) electrodes using a platinum counter electrode and a saturated calomel reference electrode (SCE). The solutions used for the electropolymerization contained 0.02 M terfuran with 0.05 M electrolyte [tetrabutylammonium (TBA<sup>+</sup>) salts of ClO<sub>4</sub><sup>-</sup>, CF<sub>3</sub>SO<sub>3</sub><sup>-</sup>, BF<sub>4</sub><sup>-</sup>, PF<sub>6</sub><sup>-</sup>, or LiClO<sub>4</sub><sup>-</sup>] in acetonitrile that was deaerated by argon bubbling. The films obtained were smooth and continuous but brittle. Cyclic voltammetric experiments were performed with a Princeton Applied Research Potentiostat/Galvanostat Model 273.

The polyfuran films exhibited a shiny surface on the platinum-grown side and a mat surface on the side facing the bulk solution. The polymer was insoluble in solvents such as nitrobenzene, propylene carbonate, acetonitrile, chloroform, tetrahydrofuran, and water. The doped polyfuran, coated on the electrode, was undoped by cathodically reducing the film to its neutral state. After undoping, the film-covered electrode was rinsed repeatedly with copious amounts of solvent and then dried under vacuum. The thickness of the polyfuran film was estimated from the relationship 7.5(1) nm/(mC cm<sup>2</sup>) which was determined from four linear plots of charge passed during electrosynthesis versus the film thickness, as measured with a Dektak surface profile system. The thickness measurements were performed on dry oxidized films containing CF<sub>3</sub>SO<sub>3</sub><sup>-</sup>, having a thickness between 50 and 1000 nm. The UV-visible spectra were recorded on Hitachi U-2000 and on Shimadzu UV/vis/NIR spectrophotometers. The FTIR spectroscopy was performed with a Nicolet 740 FTIR spectrometer, using samples prepared by grinding the polymer film with KBr and then pressing the mixture into a pellet.

The scanning electron micrographs (SEM) were obtained on a JEOL JSM-35CF microscope. X-ray photoelectron spectroscopy (XPS) was performed on a Perkin-Elmer/Physical Electronics Model 5400 ESCA system having a base pressure of  $5 \times 10^{-10}$  Torr. XPS data were obtained with a Mg or Al radiation anode. The overall energy resolution was 0.8 eV. Variable-temperature magnetic susceptibility data were collected with a Quantum Design SQUID system at various applied magnetic fields, 500–1500 G. Electron spin resonance (ESR) spectra were obtained with a Varian E-4 spectrometer. Direct current electrical conductivity and measurements of the polyfuran powder (pressed pellet) were obtained from 100 to 320 K using a data acquisition and analysis system, described elsewhere.<sup>13</sup>

### Results and Discussion

**A. Electrochemistry.** The synthetic approaches to polyfuran reported to date have yielded a material with spectroscopic and transport properties typical of a nonconjugated material.<sup>9,10</sup> This

(12) (a) Leung, W.-Y.; LeGoff, E. *Synth. Commun.* **1989**, *19*, 787. (b) Wu, C.-G.; Marcy, H. O.; DeGroot, D. C.; Schindler, J. L.; Kannewurf, C. R.; Leung, W.-Y.; Benz, M.; LeGoff, E.; Kanatzidis, M. G. *Synth. Met.* **1991**, *41/43*, 797.

(13) Lyding, J. W.; Marcy, H. O.; Marks, T. J.; Kannewurf, C. R. *IEEE Trans. Instrum. Meas.* **1988**, *37*, 76.

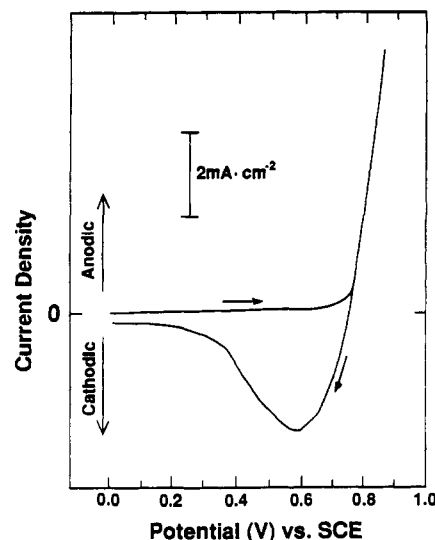


**Figure 1.** Current-voltage curve for the synthesis of a polyfuran film on a Pt electrode in acetonitrile containing 0.02 M terfuran and 0.05 M TBACF<sub>3</sub>SO<sub>3</sub>. Scan rate 50 mV/s.

departure from the expected behavior is due to the relatively drastic synthetic conditions employed. For example, electrochemical polymerization of furan requires an applied potential of >3 V vs SCE, too oxidizing an environment for the resulting polymer which deposits on the electrode. Therefore, even if the expected polymer forms initially it quickly decomposes oxidatively to a poorly defined product. We chose terfuran as the monomer in order to decrease the applied potential to a range that would be better tolerated by conjugated systems, in this case ~0.75 V. Bifuran oxidizes at a potential that was deemed still too high for the polymer, while quaterfuran was viewed as too long an oligomer to sustain extensive polymerization.<sup>12</sup> Polythiophene synthesized from other polyheterocycles such as terthiophene also forms at low oxidation potential relative to that synthesized from single thiophene.<sup>14</sup> In this work, polyfuran was synthesized electrochemically according to eq 1.

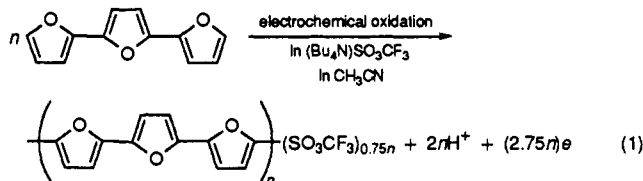


Figure 1 shows the current-voltage curve obtained during the synthesis of a polyfuran film on a Pt electrode in CH<sub>3</sub>CN containing 0.02 M terfuran and 0.05 M TBACF<sub>3</sub>SO<sub>3</sub>. Simultaneously with anodic current production, a green adhesive film forms on the surface of the Pt electrode. As the potential is swept from 0 to 0.75 V the current remains low. At electrode potentials  $\geq 0.75$  V the anodic current increases sharply and stabilizes after several seconds. While the oxidative polymerization characteristic of the monomer is independent of the dopant anion (i.e. CF<sub>3</sub>SO<sub>3</sub><sup>-</sup> is replaced by BF<sub>4</sub><sup>-</sup>, ClO<sub>4</sub><sup>-</sup>, or PF<sub>6</sub><sup>-</sup>), the color of the produced doped polymer varies with the anions used during the electropolymerization, see Table I. The color changes from green (CF<sub>3</sub>SO<sub>3</sub><sup>-</sup>) to green-brown (BF<sub>4</sub><sup>-</sup>), to reddish-orange (ClO<sub>4</sub><sup>-</sup>), to brown (PF<sub>6</sub><sup>-</sup>). This strongly suggests that the polymer structure is greatly influenced by the nature of the dopant anion (vide infra). The best quality product, possessing the longest conjugation length, is produced by CF<sub>3</sub>SO<sub>3</sub><sup>-</sup>. Upon reduction of the oxidized green film to the neutral form, the color changes to

(14) Roncali, J.; Garnier, F.; Lemaire, M.; Garreau, R. *Synth. Met.* **1986**, *15*, 323.

Table I

electrolyte (anions)	$E_{a,p}^a$ (V)	$E_{c,p}^b$ (V)	$E_{1/2(oxd)}^c$ (V)	oxidation level	color (oxd form)
CF <sub>3</sub> SO <sub>3</sub> <sup>-</sup>	0.34	0.30	0.32	0.25	green
BF <sub>4</sub> <sup>-</sup>	0.36	0.32	0.34	0.24	green-brown
ClO <sub>4</sub> <sup>-</sup>	0.60	0.54	0.57	0.08	reddish-orange
PF <sub>6</sub> <sup>-</sup>	0.74	0.70	0.72	0.05	brown

<sup>a</sup>  $E_{a,p}$  = anodic potential. <sup>b</sup>  $E_{c,p}$  = cathodic potential. <sup>c</sup>  $E_{1/2} = (E_{a,p} + E_{c,p})/2$ .

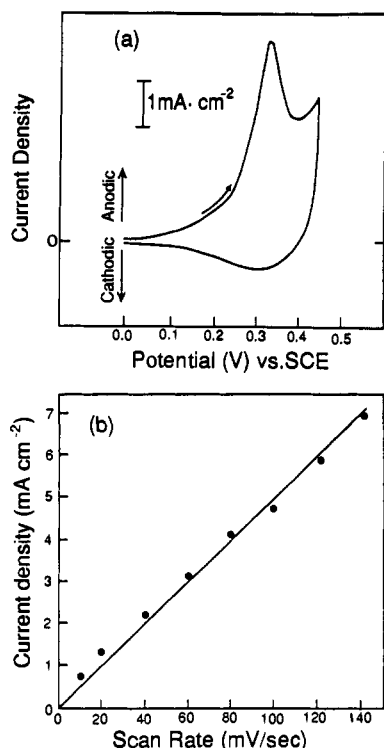


**Figure 2.** (a) Cyclic voltammogram of polyfuran film (50 nm) on a Pt electrode in acetonitrile with 0.05 M TBACF<sub>3</sub>SO<sub>3</sub>. Scan rate 50 mV/s. (b) Plot of peak current density vs the scan rate for a 100 nm thick film on a Pt electrode in acetonitrile with 0.05 M TBACF<sub>3</sub>SO<sub>3</sub>.

yellow. The reduction or undoping of the oxidized polymer occurs over a potential range of +0.75 to 0.0 V/SCE.

The cyclic voltammogram of a film (50 nm) of polyfuran on a platinum electrode in CH<sub>3</sub>CN is shown in Figure 2a. The oxidation of polyfuran is accompanied by a change of color from yellow to green which is completely reversed upon reduction to the neutral state. The redox process is found to be reversible as confirmed by Coulometric measurements during the redox process. These films can be cycled repeatedly between the oxidized and the neutral state. During oxidation charges are removed from the valence band of the polymer as the applied voltage reaches 0.20 V/SCE. This is the onset potential for the oxidation of the polymer and corresponds to the highest occupied states in the valence band. The charge that is removed from the polymer backbone electrochemically is balanced by ionic species that transfer from the electrolyte to the polymer, thus ensuring overall electrical neutrality. This association has important consequences on the length of the conjugated chains, the doping level, the chemical structure, and consequently the conductivity of this polymer, as described below. The cyclic voltammetric data of polyfuran exhibit an anodic peak at 0.34 V and a corresponding cathodic peak at 0.30 V, with a difference in peak potentials of 40 mV. This difference is commonly observed in the electrochemistry of conducting polymers (at comparable scan rates and the same dopant ions) and may be due to a number of factors including the ease of diffusion of dopant ion in and out of the film, film thickness, and reorganization of chains in the transition

between the rigid planar oxidized and flexible neutral states.<sup>15</sup> The anodic peak is noticeably sharper than the cathodic peak and the narrow peak width at half-height of 50 mV indicates a homogeneous and relatively narrow distribution of conjugation lengths along the polymer chains. From the anodic and cathodic peak potentials we determine the average potential necessary for the formation of the doped state of the polymer to be 0.32 V. The peak currents scale linearly with scan rate, as has been observed in many polythiophenes. This is seen in Figure 2b which shows a plot of peak current density,  $i_p$  in mA/cm<sup>2</sup>, against scan rates up to 140 mV/s.

Table I shows that the average potential necessary for the formation of the doped state of the polymer varies with the electrolyte used during the redox process. In increasing order they are the following: CF<sub>3</sub>SO<sub>3</sub><sup>-</sup> < BF<sub>4</sub><sup>-</sup> < ClO<sub>4</sub><sup>-</sup> < PF<sub>6</sub><sup>-</sup>. This variation reflects a strong association between the positively charged sites in the oxidized polymer and the dopant ions. In fact, spectroscopic evidence suggests that the ClO<sub>4</sub><sup>-</sup> and PF<sub>6</sub><sup>-</sup> do not even form polyfuran as shown in Chart I, but a poorly defined nonconjugated material. The strong association of these two dopants with the oxidized polymer results in irreversible chemical reactions which dramatically alter the conjugated structure. In the doped state the charge created in the conjugated system is delocalized along the polymer backbone. The longer conjugated chains lead to a better electronic delocalization, as higher energy electronic states in the valence band of the polymer are emptied. Thus, the lowest potential, associated with the CF<sub>3</sub>SO<sub>3</sub><sup>-</sup> anion, suggests the highest conjugation length for the corresponding polymer.

The electrochemical stoichiometry for the oxidation reaction was estimated based on the comparison of the Coulombic charge associated with the oxidation wave in the voltammogram to the weight of the film. This estimation was done by measuring the area of the oxidation wave in the cyclic voltammogram, which corresponds to  $3.31 \times 10^{-8}$  F/cm<sup>2</sup>, and the number of moles of monomer units on the electrode, which is estimated to be  $12.24 \times 10^{-8}$  mol/cm<sup>2</sup>. A stoichiometry of four furan rings per one electron suggests that one electron is removed from polymer segments containing four furan units. Other polymers such as polythiophene and polypyrrole exhibit doped behavior with a similar electrochemical stoichiometry of 0.25 charge/monomeric unit.<sup>16</sup>

The scanning electron micrographs of CF<sub>3</sub>SO<sub>3</sub><sup>-</sup>, BF<sub>4</sub><sup>-</sup>, ClO<sub>4</sub><sup>-</sup>, and PF<sub>6</sub><sup>-</sup>-doped polyfuran films which show a wide variation of surface morphology of these films emphasize the influence of the nature of the electrolyte anion on polymer growth. Electropolymerization produces regions in the films with different growth rates. Similar growth behavior has been observed in the case of polythiophene<sup>17</sup> and polyselenophene.<sup>4</sup> Despite the differences observed in the surface morphologies, the flotation densities of the films show little variation and lie in the range 1.31–1.35 g/cm<sup>3</sup>.

**B. Structural and Optical Properties.** Figure 3 shows the infrared spectra of terfuran and oxidized CF<sub>3</sub>SO<sub>3</sub><sup>-</sup> and BF<sub>4</sub><sup>-</sup>-doped polyfuran. The infrared spectrum of terfuran exhibits several bands characteristic of furan vibrational modes (1585, 1535, 1440, 1385, 1202, 1158, 1060, 1008, 885, 727 cm<sup>-1</sup>).<sup>18,19</sup> These bands are retained in the spectra of the polymer in both CF<sub>3</sub>SO<sub>3</sub><sup>-</sup> and BF<sub>4</sub><sup>-</sup>-doped states. The 1590-, 1510-, 1440-, and 940-cm<sup>-1</sup> bands are assigned to the vibrational modes of the furan monomer. The bands at 1164, 1088, and 1031 cm<sup>-1</sup> are ascribed

(15) Meerholz, K.; Heinze, J. *Angew. Chem., Int. Ed. Engl.* **1990**, *29*, 692.

(16) (a) Tourillon, G.; Garnier, F. *J. Phys. Chem.* **1983**, *87*, 2289. (b) Diaz, A. F.; Kanazawa, K. In *Extended Linear Chain Compounds*; Miller, J., Ed.; Plenum Press: New York, 1982; Vol. 3.

(17) Tourillon, G.; Garnier, F. *J. Polym. Sci.* **1984**, *22*, 83.

(18) Rao, C. N. R. In *Chemical Applications of Infrared Spectroscopy*; Academic Press: New York, 1963; p 317.

(19) (a) Kartitzky, A. R. *Q. Rev. Chem. Soc.* **1959**, *4*, 353. (b) Kartitzky, A. R.; Lagowski, J. M. *J. Chem. Soc.* **1959**, 657. (c) Kresta, J.; Livingston, M. K. *Polym. Lett.* **1970**, *8*, 795.

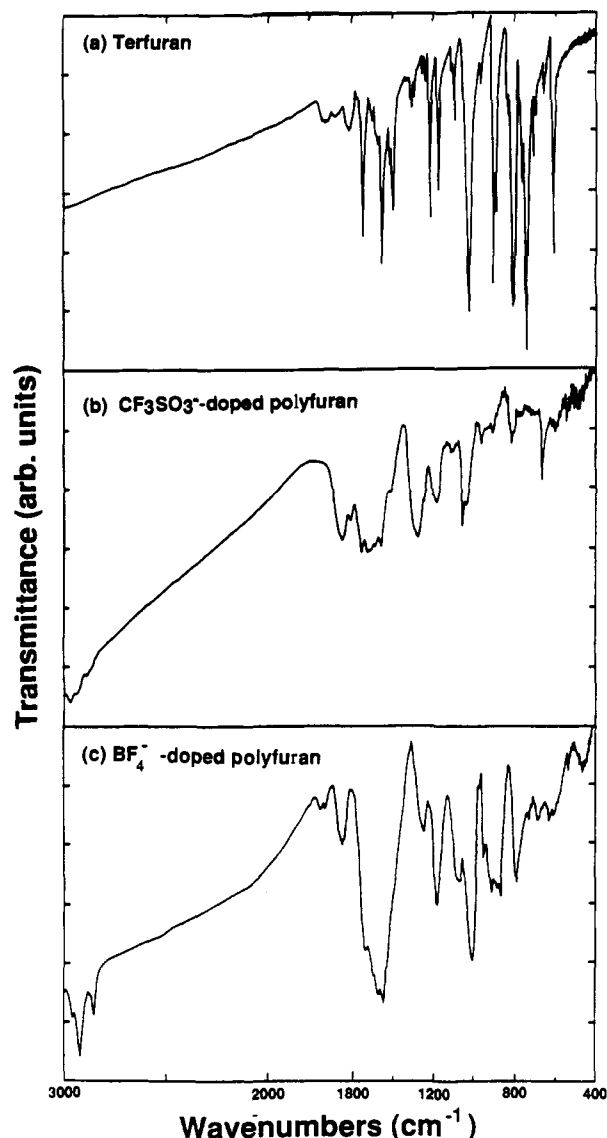


Figure 3. Infrared transmission spectra of (a) terfuran (b)  $\text{CF}_3\text{SO}_3^-$ -doped polyfuran, and (c)  $\text{ClO}_4^-$ -doped polyfuran from powder pressed in KBr.

to C–H bending and stretching modes, and the bands at 890 and 638  $\text{cm}^{-1}$  are assigned to out-of-plane bending of C–H modes. The band at 1535  $\text{cm}^{-1}$  is related to the C=C stretch of the furan monomer and the 788- $\text{cm}^{-1}$  band is characteristic of the  $\alpha, \alpha'$ -coupling of the carbon backbone.<sup>20</sup> The latter band is consistent with the linear structure shown in Chart I. The bands of  $\text{CF}_3\text{SO}_3^-$  are assigned at 1635, 1258, and 638  $\text{cm}^{-1}$ . These bands are replaced by new ones at 1010, 780, 590, and 520  $\text{cm}^{-1}$  when  $\text{CF}_3\text{SO}_3^-$  is replaced by  $\text{BF}_4^-$ <sup>21</sup> and 1100 and 625  $\text{cm}^{-1}$  for replacement by  $\text{ClO}_4^-$ . In the neutral, undoped state the bands of the anion disappear. The  $\text{BF}_4^-$  sample is decomposed. The value of 25% shown in Table II is based on how much F we find in the material by XPS measurements. However, we believe that  $\text{BF}_4^-$  no longer exists.

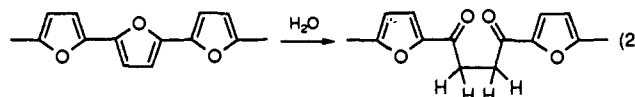
In the  $\text{BF}_4^-$ -doped polyfuran the vibrational modes at 2930 and 2850  $\text{cm}^{-1}$  are due to aliphatic C–H modes, indicating that some furan rings are saturated. These bands are substantially reduced in the  $\text{CF}_3\text{SO}_3^-$ -doped polyfuran. Furthermore, the presence of C=O modes at 1730 and 1750  $\text{cm}^{-1}$  indicates the occurrence of ring opening (see eq 2) in the  $\text{BF}_4^-$ -doped polyfuran, which is absent in  $\text{CF}_3\text{SO}_3^-$ -doped polyfuran. Equation 2 is

Table II

compound	O/C ratio per furan ring	doping level per furan ring	
		doped polymer	undoped polymer
terfuran	0.23		
polyfuran $\text{CF}_3\text{SO}_3^-$ -doped	0.28	0.26	0.00
polyfuran $\text{BF}_4^-$ -doped	0.06	0.27	0.25 ( $\text{BF}_4^-$ decomposed)
polyfuran $\text{ClO}_4^-$ -doped	0.20	0.06	0.00
polyfuran $\text{PF}_6^-$ -doped	0.26	0.04	0.03

intended to show that there is ring opening, but not its precise nature. The relatively high frequency of the C=O stretching vibrations may be due to the fact there are ring openings adjacent to one another thus destroying conjugation with the furan ring. The IR bands of the doped material are broadened and shifted to lower frequencies with respect to those of terfuran. This is due to the vibronic coupling of the delocalized positive charges in the oxidized polymer with the skeletal stretching vibrations of the carbon backbone. This effect is also observed in other conducting polymers.<sup>22</sup> The corresponding spectra of  $\text{ClO}_4^-$ - and  $\text{PF}_6^-$ -doped material show even more intense C–H and C=O stretching vibrations, confirming that significant structural changes and serious disruption of the expected conjugation length are occurring. The variation of the doping level and the difference in chemical structure result in the different colors of the doped polyfuran samples with varying dopant ions (see Table I).

The presence of absorptions characteristic of aliphatic C–H and carbonyl moieties in the vibrational spectra of polyfuran, and their strong dependence on dopant counterion, is in stark contrast with the behavior the homologous polypyrrole and polythiophene which do not show such effects. Out of the three polymers, polyfuran is the most chemically unstable, particularly in the oxidized, doped state and particularly with respect to ring opening by nucleophilic reagents. One potential pathway to ring opening could be nucleophilic attack on positively charged  $\alpha$ -carbon centers by the dopant and/or water, shown schematically in eq 2. The reason why, out of all dopant anions used,  $\text{ClO}_4^-$



and  $\text{PF}_6^-$  are the most damaging to the conjugated structure is not clear, but it is noteworthy to point out that the least damaging anion,  $\text{CF}_3\text{SO}_3^-$ , is also the least nucleophilic. This is consistent with the conclusion that doped polyfuran is highly susceptible to acid/base effects. Even for  $\text{CF}_3\text{SO}_3^-$ , a small degree of ring opening is still present and thus expected conjugation lengths, on average, will be shorter than those present in polypyrrole and polythiophene. Therefore, electrical conductivities and free carrier mobilities are expected to be considerably lower in polyfuran (see below). During electrochemical polymerization using furan or bifuran, such ring opening is extensive, due to the highly oxidizing environment (high density of positively charged  $\alpha$  carbons), and no conjugated structure is obtained.<sup>9,10</sup> We also observe that washing polyfuran with either acidic or slightly basic aqueous solution tends to substantially increase the intensities of the vibration peaks due to the carbonyl units, suggesting extensive hydrolytic ring opening is occurring.

The UV–visible absorption spectra of undoped and  $\text{CF}_3\text{SO}_3^-$ -doped polyfuran films are shown in Figure 4. The neutral polymer exhibits an absorption maximum at 468 nm. This broad absorption band, which lies between 430 (2.9 eV) and 540 nm (2.3 eV), corresponds to the  $\pi$ – $\pi^*$  interband transition. The optical properties of conjugated polymers are generally charac-

(20) Hotta, S.; Hosaka, T.; Shimotsuma, W. *J. Chem. Phys.* **1984**, *80*, 954.

(21) Bates, J. B.; Quist, A. S.; Boyd, G. E. *J. Chem. Phys.* **1971**, *54*, 124.

(22) Rabolt, J. F.; Clark, T. C.; Street, G. B. *J. Chem. Phys.* **1979**, *81*, 4615.

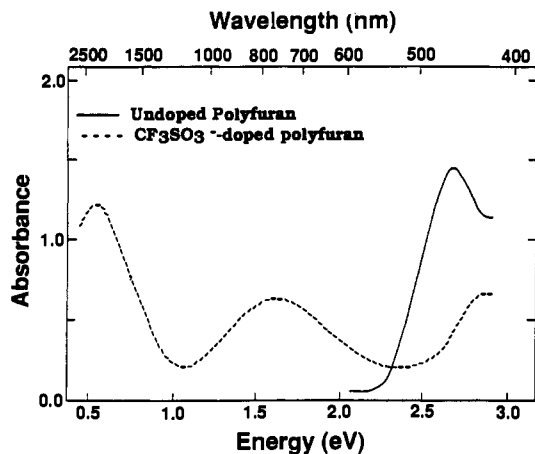


Figure 4. UV-visible spectrum of a polyfuran-coated tin-doped indium oxide (ITO) electrode: (—) undoped, (---)  $\text{CF}_3\text{SO}_3^-$ -doped.

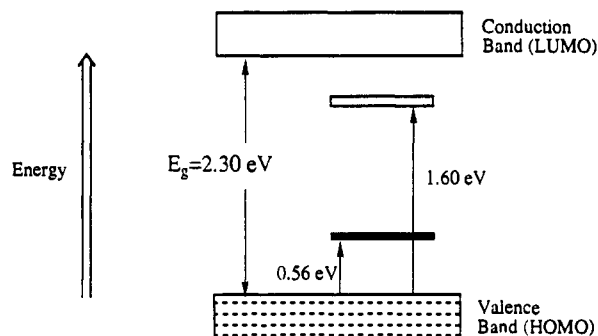


Figure 5. Electronic energy level diagram of  $\text{CF}_3\text{SO}_3^-$ -doped polyfuran.

terized by a wide absorption band due to intrinsic energetic disorder in these polymers. This disorder is produced primarily by the variation of conjugation length in polymer segments. The band gap,  $E_g$ , for a direct interband transition may be deduced from the energy absorption edge of the spectrum. Extrapolation of the plot  $(\alpha h\nu)^2$  vs  $h\nu$ , where  $\alpha$  is the absorption coefficient, yields a direct band gap of 2.35 eV. This value is larger than that reported for polythiophene (2.0 eV) and smaller than that of polypyrrole (3.2 eV) in agreement with theoretical calculations.<sup>23</sup>

The passage from the undoped to the doped state is accompanied by weakening and blue shift of the absorption band in the visible region and the appearance of two absorption features in the near-IR region. The two subgap levels at 775 (1.60 eV) and 2200 nm (0.56 eV) are attributed to bipolaronic transitions between band gap states which arise as a consequence of electronic coupling with the polymer backbone.<sup>24</sup> Figure 5 provides a summary of the energy level diagram of the  $\text{CF}_3\text{SO}_3^-$ -doped polyfuran. The polymer has a 2.35-eV band gap between the highest occupied molecular orbital (HOMO) and the lowest unoccupied molecular orbital (LUMO). In the band gap two bipolaron states are formed, which are located 0.56 (low-energy localized state) and 1.60 eV (high-energy localized state) from the valence band.

**C. X-ray Photoelectron Spectroscopy (XPS).** For better understanding of the electronic properties of polyfuran, which are related strongly to the chemical structure of the polymer backbone, we investigated this polymer with X-ray photoelectron spectroscopy. The O/C atomic ratio, the doping level of  $\text{CF}_3\text{SO}_3^-$ ,  $\text{BF}_4^-$ ,  $\text{ClO}_4^-$ , and  $\text{PF}_6^-$ -doped polyfuran, and the O/C atomic ratio of undoped polyfuran and terfuran are displayed in Table II. The value of O/C = 0.26 found for undoped polyfuran, initially

(23) Hernandez, V.; Lopez-Navarrete, J. T.; Marcos, J. L. *Synth. Met.* **1991**, *41/43*, 489. Bakhshi, A. K.; Ladik, J.; Seel, M. *Phys. Rev. B* **1987**, *35*, 704.

(24) (a) Bredas, J. L.; Themas, B.; Fripiat, J. G.; Andre, J. M.; Chance, R. R. *Phys. Rev. B* **1984**, *29*, 6761. (b) Scott, J. C.; Pfluger, P.; Kroundi, M. T.; Street, G. B. *Phys. Rev. B* **1983**, *28*, 2140.

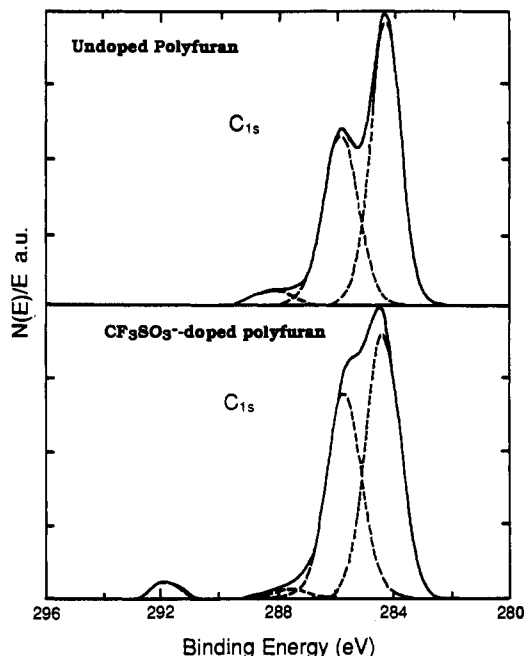


Figure 6.  $\text{C}_{1s}$  core level spectra of (a) undoped and (b)  $\text{CF}_3\text{SO}_3^-$ -doped polyfuran films. The features through the data correspond to the fitting with Gaussian functions.

synthesized in the presence of  $\text{CF}_3\text{SO}_3^-$ , agrees well with the theoretical value expected according to the formula of Chart I. In contrast, the 0.06 O/C ratio of  $\text{BF}_4^-$ -doped polyfuran indicates that the polymer does not have the same structural features as the monomer due to ring opening of furan.

Figure 6 shows the  $\text{C}_{1s}$  line shape of a 200 nm thick polyfuran film in the undoped and  $\text{CF}_3\text{SO}_3^-$ -doped state. The  $\text{C}_{1s}$  peak can be decomposed into three features. The feature at 284.42 eV with a line width of 1.22 eV is due to  $\beta$  carbons, while the feature at 285.86 eV, with a line width of 1.37 eV, is due to  $\alpha$  carbons of the furan ring. The resulting area of  $\alpha$  carbons is slightly larger than that of  $\beta$  carbons. This is attributed to structural deviations from the ideal  $\pi$ -conjugated system and to the presence of defects which affect the  $\beta$  carbons more than the  $\alpha$  carbons. The 1.30-eV splitting of the  $\text{C}_{1s}$  levels is due to the chemical difference between  $\alpha$  and  $\beta$  carbons in the individual furan units.<sup>25</sup> The third weak feature at 288.18 eV located 2.33 eV above the  $\alpha$  carbon peak is attributed either to structural disorder in the polymer film due to cross-linking and chain termination<sup>26</sup> or to "shake-up" which involves  $\pi$ - $\pi^*$  transitions between the highest occupied valence levels and the lowest unoccupied bands.<sup>27</sup> In the latter case this value corresponds to band-gap photoexcitation and is consistent with the 2.35-eV band gap deduced by UV-visible absorption measurements described above. In the doped state the peak located at 291.88 eV is due to the C-F bonds present in the dopant.

The  $\text{O}_{1s}$  core level line, see Figure 7, in the undoped sample exhibits two distinct features, one at 533.88 eV, corresponding to  $\text{O}_{1s}$  of the furan ring, and one at 531.94, originating from the  $\text{O}_{1s}$  of residual  $\text{CF}_3\text{SO}_3^-$  anion. In the doped samples, the height of this peak substantially increases due to the presence of  $\text{CF}_3\text{SO}_3^-$  anion in the polymer backbone. The widths of the  $\text{C}_{1s}$  and  $\text{O}_{1s}$  peaks are broader compared to those of the undoped samples (see Table III). This broadening is due either to modification of

(25) Siegbahn, K.; Nordling, C.; Fahlman, A. In *ESCA, Atomic Molecular and Solid State Structure Studied by Means of Electron Spectroscopy*; Almqvist and Wiksells: Uppsala, 1967.

(26) Pfluger P.; Street, G. B. *J. Chem. Phys.* **1984**, *80*, 544.

(27) (a) Salaneck, W. R.; Erlandsson, R.; Prejza, J.; Lundstrom, I.; Duke, G. B.; Ford, W. K. *Polym. Prepr.* **1982**, *23*, 120. (b) Salaneck, W. R.; Erlandsson, R.; Prejza, J.; Lundstrom, I.; Inganas, O. *Synth. Met.* **1983**, *5*, 125.

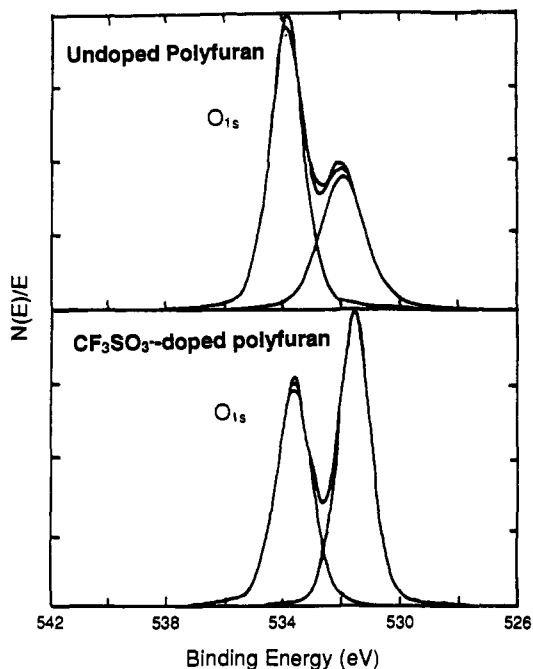


Figure 7. O<sub>1s</sub> core level spectra of (a) undoped and (b) CF<sub>3</sub>SO<sub>3</sub><sup>-</sup>-doped polyfuran.

Table III

polymer	C <sub>α</sub> 1s, fwhm (eV)	C <sub>β</sub> 1s, fwhm (eV)	C <sub>γ</sub> 1s, fwhm (eV)	O1s, fwhm (eV)
polyfuran undoped	285.86, 1.37	284.32, 1.22	288.18, 1.60	533.88, 1.36
polyfuran doped	285.72, 1.40	284.40, 1.40	287.60, 1.60	533.64, 1.45

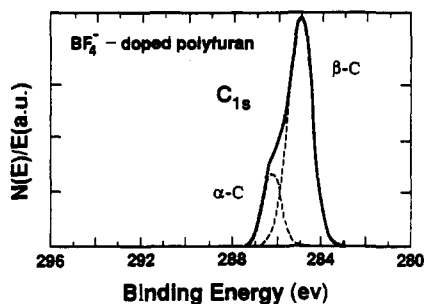
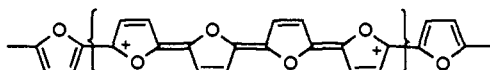


Figure 8. C<sub>1s</sub> core level spectrum of BF<sub>4</sub><sup>-</sup>-doped polyfuran. The more intense peak is due to the β carbons.

electronic structure of the polymer during the doping process, associated with narrowing of the band gap toward the Fermi level,<sup>28</sup> or to the transformation of the polymer chain during the doping process from the aromatic into the quinoid-like structure associated with the appearance of localized bipolaron states in the band gap:<sup>24</sup>



In the C<sub>1s</sub> core level spectrum of the BF<sub>4</sub><sup>-</sup>-doped polyfuran, see Figure 8, the β carbons possess a much larger area (4:1) than the α carbons. This significant deviation from the expected ratio is related to ring opening of furan repeating units, which heavily disrupts the π-conjugated system of the polymer backbone. These data support the infrared spectroscopic data presented above.

**D. Magnetic Properties.** Polyfuran was studied by magnetic susceptibility and electron resonance spectroscopy (ESR) mea-

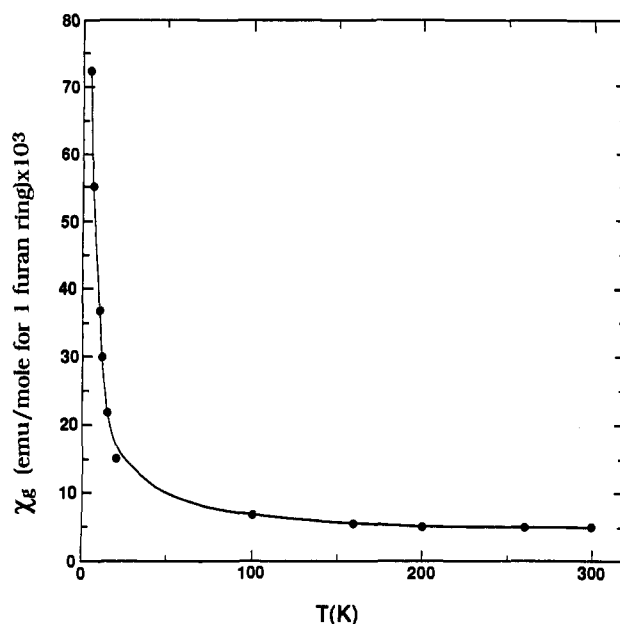


Figure 9. Temperature dependence of magnetic susceptibility of CF<sub>3</sub>SO<sub>3</sub><sup>-</sup>-doped polyfuran.

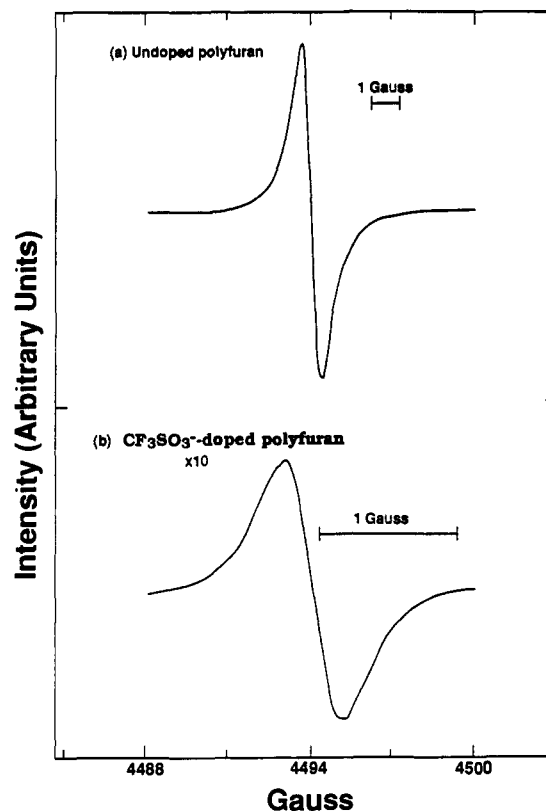


Figure 10. ESR spectra of (a) undoped and (b) CF<sub>3</sub>SO<sub>3</sub><sup>-</sup>-doped polyfuran. Figure 9 displays magnetic susceptibility data versus temperature for the CF<sub>3</sub>SO<sub>3</sub><sup>-</sup>-doped polymer. At room temperature the magnetic susceptibility corresponds to  $5.3 \times 10^{-3}$  emu/mol per furan ring. The susceptibility can be decomposed into a temperature-independent Pauli susceptibility component, for temperatures above 200 K, and a Curie-Weiss law component which becomes dominant at lower temperatures and is due to the presence of free radicals on the polymer backbone (see below).

Figure 10 shows the room temperature ESR spectra of the undoped and the CF<sub>3</sub>SO<sub>3</sub><sup>-</sup>-doped polyfuran. The undoped polymer exhibits a Gaussian signal which changes to an intermediate line shape between Gaussian and Lorentzian upon doping. The Gaussian ESR signal is attributed to the presence of localized

spins and the Lorentzian nature of the signal indicates that some spin originates from mobile charges. The peak-to-peak line width ( $\Delta H_{pp}$ ) is 0.8 G for the undoped and 0.45 G for the doped polymer. The spin concentration decreases from  $8.4 \times 10^{19}$  spins/mol in the undoped sample to  $5.1 \times 10^{19}$  spins/mol in the doped sample. The undoped and doped polyfuran films have  $g$  values of 2.0010 and 2.0019, respectively, indicating that the species responsible for the ESR signal originates principally from unpaired electrons in the conjugated  $\pi$ -electron system of the carbon backbone. The unpaired electrons in the undoped material come from defects in the polymer, as is typically seen in most undoped conjugated polymers. Furthermore, the absence of a  $g$ -value anisotropy indicates that charge transport occurs along the  $\pi$ -conjugated system of the carbon backbone and that O contributes negligibly to the spin resonance.<sup>29</sup> These results suggest that the large increases in electrical conductivity, described below, cannot result from unpaired spins. These data support the formation of polaron and bipolaron states with localized intragap levels. In the neutral state or low doped state, polaron ( $\text{spin } 1/2$ ) energy states give rise to intragap localized levels. At higher doping levels the polaron states combine with each other to form spinless bipolaron states, localized again within the gap. This explanation is in good agreement with theoretical calculations,<sup>24</sup> which predict the formation of bonding and antibonding bipolaron bands within the band gap of the polymer. It is also in agreement with the observed optical spectra.

**E. Electrical Conductivity Studies.** The room temperature electrical conductivity of polyfuran films varies over a range of  $10^9$  S/cm between the undoped and the  $\text{CF}_3\text{SO}_3^-$ -doped states. In the undoped state the conductivity of polyfuran was  $10^{-11}$  S/cm. The highest electrical conductivity obtained in the doped state ( $\text{CF}_3\text{SO}_3^-$ ) of the polymer was  $2 \times 10^{-3}$  S/cm. Similar conductivities ( $10^{-2}$  S/cm) have been reported in the case of polythiophene synthesized from terthiophene, and this was attributed to the increased stability of the radical cations formed from terthiophene and the low molecular weights of the resulting polymers.<sup>14</sup> However, in this case the low conductivity may also be due, to a certain degree, to the expected lower degree of backbone conjugation relative to polythiophene and, of course, cross linking. This can be caused by occasional furan ring opening. It is noteworthy to point out that the electrical conductivity of the polymer reported here is the highest ever reported for polyfuran which supports the conclusion that, this time, a significantly more regular  $\pi$ -conjugated polymer has been achieved.

The anion used during the electropolymerization also has a crucial influence on the electrical conductivity. The room temperature electrical conductivity of  $\text{ClO}_4^-$ -doped polyfuran is  $10^{-4}$  S/cm. Substantially lower conductivities, of the order of  $10^{-7}$  S/cm, were obtained with the  $\text{BF}_4^-$ - and  $\text{PF}_6^-$ -doped polymers. The lower conductivities with these anions arise from the structural changes mentioned above (i.e. ring-opening and disruption of conjugation in the resulting material).

The temperature dependence of the electrical conductivity over the temperature range from 160 to 320 K is shown in Figure 11. The strong temperature dependence indicates a thermally activated process. The conductivity decreases with temperature, characteristic of a semiconductor-like material.<sup>30</sup> The data show that two different charge transport regimes exist over the temperature range measured. A plot of  $\log \sigma$  versus  $1/T$  in the high-temperature range (320–250 K) gives a linear dependence from the slope of which an activation energy of 0.33 eV is obtained. A similar plot in the low-temperature range (250–160 K) also gives a linear dependence corresponding to an activation energy of 0.16 eV. This thermal activation energy in conjugated polymers can be viewed as the average ionization energy required to promote

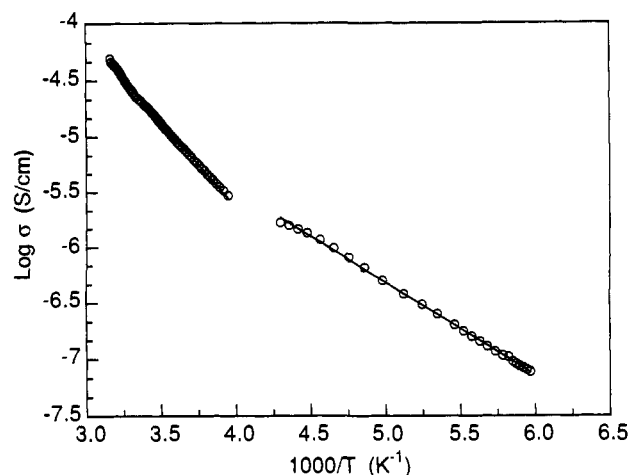


Figure 11. Temperature dependence of electrical conductivity of pressed pellets of  $\text{CF}_3\text{SO}_3^-$ -doped polyfuran. Least-squares linear fits are drawn through the high-temperature and low-temperature data, respectively.

a trapped carrier to the extended state and corresponds to the trap depth. The origin of the thermally activated transport process can be multifold, such as thermal emission from structural defects and/or traps,<sup>31</sup> grain boundaries, or hopping between domain-like formations of conducting regions of the polymer chains.<sup>32</sup> The different activation energies in the high- and low-temperature regions arise from the fact that different processes for thermally activated transport become dominant as the temperature changes. Thus, depending on the temperature range, two different conductivity mechanisms seem to dominate.

## Conclusions

Prior to this work polyfuran had been among the most ill-defined of conjugated polymers. We have demonstrated that good quality polyfuran films have been grown in large amounts electrochemically under mild conditions by using terfuran as the monomer for polymerization. The electrochemical and physical properties of the polymer depend on the nature of the electrolyte used during synthesis. Among  $\text{BF}_4^-$ ,  $\text{PF}_6^-$ ,  $\text{ClO}_4^-$ , and  $\text{CF}_3\text{SO}_3^-$ , the last anion yields the highest quality polymer in which the basic furan ring is largely retained within the polymeric structure. Substantial structural deviations from the ideal conjugated polyfuran structure (e.g. furan ring opening and saturation) were observed with the other four anions. This work shows that furan ring opening is the major cause of deterioration of polyfuran which is brought about by moisture in basic or acidic environments. Polyfuran exhibits thermally activated conductivities of  $2 \times 10^{-3}$  S/cm, at room temperature, in the oxidized  $\text{CF}_3\text{SO}_3^-$ -doped state. Bipolarons are found to be the nature of charge storage in the doped polyfuran. On the basis of the properties of  $\text{CF}_3\text{SO}_3^-$ -doped polyfuran we conclude that this material comes closest to possessing the idealized structure shown in Chart I than any other polyfuran reported to date.

**Acknowledgment.** Financial support from the National Science Foundation (DMR-89-17805) is gratefully acknowledged. M.G.K. is an A. P. Sloan Fellow, 1991–1993. Partial funding from the Beckman Foundation is also acknowledged. At Northwestern University this work made use of Central Facilities supported by NSF through the Materials Research Center (DMR-91-20521). We thank Rabin Bissessur for help with the ESR spin quantitation.

(29) Carrington, A.; McLachlan, A. D. In *Introduction to Magnetic Resonance*; Harper and Row: New York, 1967; Chapter 9.

(30) Mott, N. F.; Davis, E. A. In *Electronic Processes in Noncrystalline Materials*; Clarendon: Oxford, 1979; Chapter 2.

(31) Mott, N. F. *Philos. Mag.* **1969**, *19*, 825.

(32) Zuo, F.; Angelopoulos, M.; MacDiarmid, A. G.; Epstein, A. J. *Phys. Rev. B* **1987**, *36*, 3475.